Satellite Relative Motion SDRE-based Control for Capturing a Noncooperative Tumbling Object

Mahdi Akhloumadi
Moscow Institute of Physics and Technology
Moscow, Russia
akhloumadi@gmail.com

Danil Ivanov
Keldysh Institute of Applied Mathematics RAS
Moscow, Russia
ORCID: 0000-0002-8253-7092

***Abstract* — The paper considers the problem of relative motion control for a docking to the noncooperative tumbling object. The translational motion is assumed to be controlled by the thrusters; the attitude control system is based on the reaction wheels. The SDRE-based coupled motion control algorithm is proposed and its performance is studied. The misalignment of the thrusters and the reaction wheels saturation are taken into account in the numerical simulations. The area of acceptable the control system parameters for successful docking is obtained. The influence of the tumbling object angular velocity and its inertia moment ratio to the reaction wheels saturation is studied using multiple simulations.**

Keywords — control algorithm, docking, reaction wheels saturation

I. INTRODUCTION

Inactive satellites or its fragments, rocket stages on the Earth's orbit are classified as space debris. Their removal became a crucial international problem. There is a set of approaches to address this problem. Self-removal and active-removal are the main two categories of the proposed solutions [1], [2]. In the case of self-removal, the satellites are to be deorbited using its own propulsion system or external forces, e.g. aerodynamic drag, solar pressure etc. Active removal is a wide range of methods that suggest special missions for de-orbiting the noncooperative objects. These missions assume that a special satellite is to be attached to the space debris using electro dynamic tether [3], tethered space-tug [4]–[7], nets [8] or robotic arms [9], [10] to capture objects for delivering it into the lower orbit for further aerodynamic drag deorbiting. One of the crucial problem related to active space debris removal is the rendezvous, docking and capturing the non-cooperative tumbling target. Generally, onboard propulsion is used to achieve the required proximity about the debris while the required for capturing relative attitude is obtained with help of the attitude control system that could include the reaction wheels. However, the reaction wheels could saturate because of onboard thrusters misalignment or high angular velocity of tumbling object which attitude must be tracked for capturing. The paper addresses this problem.

The problem of an autonomous docking between a controlled rigid spacecraft and an uncontrolled tumbling target is well studied in the literature. In the last decade significant achievements have been obtained in the field of optimal docking control strategies. In the papers [11], [12] the model predictive control is applied to the problem. It allows to generate the safe and fuel-optimal rendezvous trajectories that guarantee collision avoidance. Its computation requires the use of convex linear and quadratic programming. In the papers [13], [14] proposed a second-order cone-programming-based methodology to solve the rendezvous and proximity operations problem. Another approach is to apply the inverse dynamics in the virtual domain method for rapid sub-optimal docking trajectory generation [15]. The fuel-optimal trajectory generation algorithms are computationally intensive, its implementation in a real-time system is very challenging. Another approach is to use non-optimal docking trajectory generation as in [16], [17] for the sake of simpler computations. In that paper State Dependent Riccati Equation (SDRE) control approached is applied for the rendezvous problem that does not require the trajectory calculation and leads to the docking points matching.

The aim of the study is to develop a control algorithm for translational and rotational motion of spacecraft to achieve the necessary relative state for the following capturing. Another main point is to investigate dynamical conditions of the uncooperative object under which it is possible to capture it with the given parameters of control system such as maximal reaction wheels angular momentum, misalignment of thrusters and weighing parameters of control algorithm. Due to nonlinearity of the coupled relative translational and angular motion models the SDRE control approached is applied. SDRE control provides sufficient optimality, stability, real-time implement ability and inherent robustness to the states and system uncertainties and disturbances [18].

The main characteristic of SDRE method is state vector factorization of nonlinear system to establish a linear-liked dynamic model with matrix of state dependent coefficients and states. There are various ways of solving SDRE for instance Theta-D, power series, and solving Algebraic Riccati equation in each integrating time step [18]. These iterative methods are time consuming and increase computational cost as a result they cannot be a proper choice for real time implementation. Consequently, investigating of a direct algorithm to solve algebraic Riccati equation is needed. An analytical way of solving state dependent Riccati equation is based on Schur decomposition algorithm. This method uses eigenvalues and their corresponding eigenvectors of Hamiltonian matrix to solve Algebraic Riccati Equation. The method is shown to be computationally faster than the iterative methods [19] and applied in this work.

The first section of the paper is devoted to problem statement. The used coordinate systems are presented and relative translational and angular motion models are described. The basics on the SDRE control are given in the second section. In the third section the results of the numerical study of the proposed algorithm are presented.

II. PROBLEM STATEMENT

A. Reference Frames

In order to derive the equations of relative motion of the chaser and the target satellites the following coordinate systems are used as presented in Fig. 1 : $\mathcal{I}$ stands for the

Earth centered inertial, Cartesian right hand reference frame with axes X,Y and Z; $\mathcal{D}$ stands for a local-vertical, local horizontal (LVLH) Euler-Hill reference frame which is fixed to the center of mass of debris with axes: $\hat{x}_{\mathcal{D}}$ is aligned with spacecraft radius-vector, $\hat{z}_{\mathcal{D}}$ is in the direction of orbital angular momentum and $\hat{y}_{\mathcal{D}}$ completes the system. Cartesian body-fixed reference frame $\mathcal{C}$ attached to the Chaser spacecraft's center of mass. It is assumed that orbital reference frames $\mathcal{D}$ is aligned with the Cartesian body-fixed reference frame of the debris.

B. Equations of motion

Nonlinear Relative translational equation of motion is in the given form [19]:

$$\begin{aligned} &\ddot{x} - 2\omega_{OT}\dot{y} - \dot{\omega}_{OT} y - 3\omega_{OT}{}^2 x = a_x + F_x, \\ &\ddot{y} + 2\omega_{OT}\dot{x} + \dot{\omega}_{OT} x = a_y + F_y, \\ &\ddot{z} + \omega_{OT}^2 z = a_z + F_z. \end{aligned} \tag{1}$$

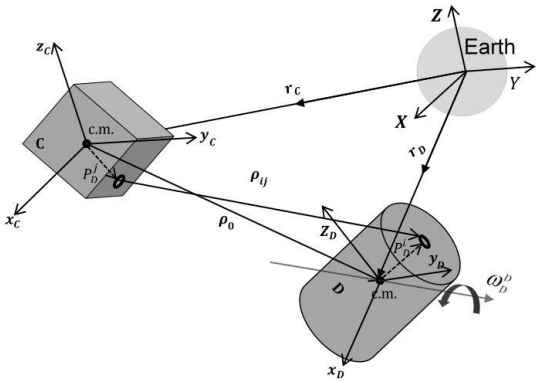

Fig. 1. Reference frames attached to spacecraft, target and earth

Here x, y, z are relative positions, ω_{OT} is the orbital angular velocity of the target, vectors **a** and **F** are produced translational control acceleration and external forces respectively.

Relative attitude of spacecraft with respect to the debris can be described using relative quaternions and angular velocities. Consider relative angular velocity vector $\boldsymbol{\omega}$ as:

$$\boldsymbol{\omega} \triangleq \boldsymbol{\omega}_C - \boldsymbol{\omega}_D. \tag{2}$$

Here $\boldsymbol{\omega}_C$, $\boldsymbol{\omega}_D$ are target and chaser angular velocities correspondingly. Four dimensional quaternion vector $\mathbf{q}$ is used to describe the relative attitude of spacecraft with respect to debris:

$$\mathbf{q} = [q_1 q_2 q_3 q_4]^T, \tag{3}$$

where q_1, q_2, q_3 are the components of the vector part of the quaternion, and q_4 is the scalar part.

The relative kinematics is expressed by the following equations in terms of relative quaternion (4):

$$\dot{\mathbf{q}} = \frac{1}{2} Q(q) \boldsymbol{\omega}^C, \tag{4}$$

where $\boldsymbol{\omega}^C$ is relative angular velocity expressed in chaser reference frame and $Q(q)$ is as follows:

$$Q = \begin{bmatrix} q_4 & -q_3 & q_2 \\ q_3 & q_4 & -q_1 \\ -q_2 & q_1 & q_4 \\ -q_1 & -q_2 & -q_3 \end{bmatrix}. \tag{5}$$

To determine the attitude of the spacecraft with respect to the debris target in $\mathcal{D}$ reference frame it is necessary to obtain time derivatives of angular velocities and use change of angular momentum equations for both debris and spacecraft. To accomplish this task by differentiating (2) one can obtain:

$$\left.\frac{d\boldsymbol{\omega}}{dt}\right|_{\mathcal{I}} = \left.\frac{d\boldsymbol{\omega}_C}{dt}\right|_{\mathcal{I}} - \left.\frac{d\boldsymbol{\omega}_D}{dt}\right|_{\mathcal{I}}. \tag{6}$$

It can be shown that (6) can be written in the following form:

$$\begin{aligned} I_D \left(\left.\frac{d\boldsymbol{\omega}}{dt}\right|_D\right)^{\mathcal{D}} = I_D M(\mathbf{q}) \left(\left.\frac{d\boldsymbol{\omega}_C}{dt}\right|_C\right)^{\mathcal{C}} - \\ - I_D \left(\left.\frac{d\boldsymbol{\omega}_D}{dt}\right|_D\right)^{\mathcal{D}} + \boldsymbol{\omega}^{\mathcal{D}} I_D (\boldsymbol{\omega}_D)^{\mathcal{D}}, \end{aligned} \tag{7}$$

where $M(\mathbf{q})$ is the transition matrix from chaser reference frame to a target reference frame, I_D is debris tensor of inertia. Furthermore the dynamical equations for the chaser and target have the following forms:

$$\left.\frac{d\mathbf{H}_C}{dt}\right|_{\mathcal{I}} = \left.\frac{d\mathbf{H}_C}{dt}\right|_C + \boldsymbol{\omega}_C \times \mathbf{H}_C = \mathbf{N}_C + \mathbf{T}_C, \tag{8}$$

$$\left.\frac{d\mathbf{H}_D}{dt}\right|_{\mathcal{I}} = \left.\frac{d\mathbf{H}_D}{dt}\right|_D + \boldsymbol{\omega}_D \times \mathbf{H}_D = \mathbf{N}_D + \mathbf{T}_D, \tag{9}$$

where $\mathbf{H}_C$ and $\mathbf{H}_D$ are angular momentums of the chaser and target, $\mathbf{N}_C$ and $\mathbf{N}_D$ are external torques acting on the spacecraft and debris respectively, and $\mathbf{T}_C$ and $\mathbf{T}_D$ are control torques. The chaser satellite is equipped with reaction wheels, so its angular momentum are calculated as follows:

$$\mathbf{H}_C = I_C \boldsymbol{\omega}_C + \mathbf{h}_{WC}, \quad \mathbf{H}_D = I_D \boldsymbol{\omega}_D, \tag{10}$$

where $\mathbf{h}_{WC}$ is the angular momentum produced by reaction wheels. Then the dynamical equation can be rewritten as follows:

$$\begin{aligned} I_C \left.\frac{d\boldsymbol{\omega}_C}{dt}\right|_{\mathcal{I}} = I_C \left.\frac{d\boldsymbol{\omega}_C}{dt}\right|_C + \dot{\mathbf{h}}_{WC} + \\ + \boldsymbol{\omega}_C I_C \boldsymbol{\omega}_C + \boldsymbol{\omega}_C \mathbf{h}_{WC} = \mathbf{N}_C + \mathbf{T}_C, \end{aligned} \tag{11}$$

$$I_D \left.\frac{d\boldsymbol{\omega}_D}{dt}\right|_{\mathcal{I}} = I_D \left.\frac{d\boldsymbol{\omega}_D}{dt}\right|_D + \boldsymbol{\omega}_D I_D \boldsymbol{\omega}_D = \mathbf{N}_D + \mathbf{T}_D. \tag{12}$$

Using equations (11), (12) and (7) and substuting $\boldsymbol{\omega}_C^C = M(q)^{-1}\left(\boldsymbol{\omega}^{\mathcal{D}} + \boldsymbol{\omega}_D^{\mathcal{D}}\right)$, $\mathbf{T}_D = 0$ (since the target object

is uncontrolled space debris), will lead to relative rotational equation of motion [19]:

$$I_D \dot{\boldsymbol{\omega}}^{\supset} = I_D M(\mathbf{q}) I_C^{-1}\mathbf{S} - I_D \boldsymbol{\omega}_D^{\supset}\boldsymbol{\omega}^{\supset} + [\boldsymbol{\omega}_D^{\supset} I_D \boldsymbol{\omega}_D^{\supset}],$$

where

$$\mathbf{S} = -M(\mathbf{q})^{-1}\left(\boldsymbol{\omega}^{\supset} + \boldsymbol{\omega}_D^{\supset}\right) I_C M(\mathbf{q})^{-1}\left(\boldsymbol{\omega}^{\supset} + \boldsymbol{\omega}_D^{\supset}\right) - \\ - M(\mathbf{q})^{-1}\left(\boldsymbol{\omega}^{\supset} + \boldsymbol{\omega}_D^{\supset}\right)\mathbf{h}_{WC} - \dot{\mathbf{h}}_{WC} + \mathbf{T}_C + \mathbf{N}_C + \mathbf{N}_D. \quad (13)$$

In the final approaching phase to the debris, when the spacecraft and object are in the vicinity of each other, the relative distance become comparable to the objects size. In this phase the spacecraft and the debris can no longer be assumed as point masses. At this stage, the geometrical properties of spacecraft and the debris affect the relative translational motion between off-centered points. The less the relative distance, the more the effect is influential. Two arbitrary points that may represent the robotic arm and specific grabbing point on the debris are shown in Fig. 1.

Assume that for capturing the debris these two points have to coincide with each other. Consider the vector $\mathbf{P}_D^{\mathbf{j}} = [P_{xD}^j, P_{yD}^j, P_{zD}^j]$ that directed from the center of mass of debris $\mathbf{P}_D^0 = [0,0,0]$ to point $\mathbf{P}_D^j$ and vector $\mathbf{P}_{\mathbf{C}}^{\mathbf{i}} = [P_{xC}^i, P_{yC}^i, P_{zC}^i]$ that directed from the spacecraft's center of mass $\mathbf{P}_C^0 = [0,0,0]$ to the point $\mathbf{P}_C^i$. Vector $\boldsymbol{\rho}_{ij}$ stands for the relative position between these two given points as presented in Fig. 1. It can be calculated as follows:

$$\boldsymbol{\rho}_{ij} = \boldsymbol{\rho}_0 + \mathbf{P}_C^i - \mathbf{P}_D^j. \quad (14)$$

The relative velocity and relative accelerations in reference frame $\supset$ can be obtained as:

$$\dot{\boldsymbol{\rho}}_{ij} = \dot{\boldsymbol{\rho}}_0 + \boldsymbol{\omega} \times \mathbf{P}_C^i, \quad (15)$$

$$\ddot{\boldsymbol{\rho}}_{ij} = \ddot{\boldsymbol{\rho}}_0 + \dot{\boldsymbol{\omega}} \times \mathbf{P}_C^i + \boldsymbol{\omega} \times \left(\boldsymbol{\omega} \times \mathbf{P}_C^i\right). \quad (16)$$

Instead of a simple uncoupled Clohessy-Whiltshire equations (1) a more general relative rotation equation of motion for two arbitrary points can be derived using the (14)-(16) [20]:

$$\begin{aligned} &\ddot{x}_{ij} - 2\omega_{OT}\dot{y}_{ij} - \dot{\omega}_{OT} y_{ij} - 3{\omega_{OT}}^2 x_{ij} = a_x + p_x, \\ &\ddot{y}_{ij} + 2\omega_{OT}\dot{x}_{ij} + \dot{\omega}_{OT} x_{ij} = a_y + p_y, \\ &\ddot{z}_{ij} + \omega_{OT}^2 z_{ij} = a_z + p_z. \end{aligned} \quad (17)$$

Here vector $\mathbf{p} = \left[p_x, p_y, p_z\right]^T$ is obtained using equations (16) and (13). It is highly coupled nonlinear term, that is rather bulky to present it in the paper, but it can be found in [19]. Thus, the problem statement of the paper is as follows. Using nonlinear coupled motion equation (17) it is required to develop a control algorithm using reaction wheels and thrusters for capturing the object, i.e. to match two body-fixed points. It is needed to obtain the area of the acceptable parameters values for successful capturing the object taking into account reaction wheels angular momentum constraints, thrusters direction misalignments relative the center of mass and debris tumbling motion.

III. SDRE-BASED CONTROL ALGORYTHM

In the paper, the application of the SDRE-based control algorithm is considered. In this section a short basics on this control methods is presented and the problem of the Riccati equation solution is addressed.

A. SDRE control method basics

While linear quadratic regulator can be used to minimize the corresponding cost function of a linear dynamical system, it may fail to address nonlinear control problem. There are cases where accuracy is of a great importance and cannot be underestimated. Nonlinear regulator approach can cover this issue. The method is proved to be stable and in some sense robust. Consider the following nonlinear system:

$$\dot{\mathbf{x}} = \mathbf{f}\left(\mathbf{x}(t)\right) + \mathbf{g}\left(\mathbf{x}(t), \mathbf{u}(t)\right), \quad (18)$$

Where $\mathbf{x}(t)$ and $\mathbf{u}(t)$ are the state and control vectors correspondingly, $\mathbf{f}$ is the nonlinear function, representing the free motion, $\mathbf{g}$ is control dependent nonlinear function. Let the system has the following initial condition:

$$\begin{aligned} &\mathbf{x}(0) = \mathbf{x}_0, \\ &f\left(\mathbf{x}(0)\right) = 0. \end{aligned} \quad (19)$$

The cost function J can be defined as:

$$J = \frac{1}{2}\int_0^{t_f} \left[\mathbf{x}(t)^T Q\, \mathbf{x}(t) + \mathbf{u}(t)^T R\, \mathbf{u}(t)\right] dt, \quad (20)$$

where Q and R are the weighting matrices. The nonlinear system can be factorized as (21) to provide a state space form. This is called a state dependent parameterization of the dynamics. The factorization is not unique for the systems of ranks bigger than one. The resulted linearized system can be treated as linear system:

$$\begin{aligned} &f(\mathbf{x}) = A(\mathbf{x})\mathbf{x}, \\ &g(\mathbf{x},\mathbf{u}) = B(\mathbf{x},\mathbf{u})\mathbf{u}. \end{aligned} \quad (21)$$

It is possible to form Hamiltonian to derive optimality conditions for the nonlinear quadratic regulator problem. According to [18] the final SDRE has the following form:

$$P(\mathbf{x},\mathbf{u})A(\mathbf{x}) + A^T(\mathbf{x})P(\mathbf{x},\mathbf{u}) - \\ - P(\mathbf{x},\mathbf{u})B(\mathbf{x},\mathbf{u})R^{-1}B^T(\mathbf{x},\mathbf{u})P(\mathbf{x},\mathbf{u}) + Q = 0. \quad (22)$$

And the control is as follows:

$$\mathbf{u}(\mathbf{x}) = -R^{-1}B^T(\mathbf{x},\mathbf{u})P(\mathbf{x},\mathbf{u})\mathbf{x}. \quad (23)$$

B. Solver of SDRE

Eeigenvalues of an associated Hamiltonian matrix can be used for obtaining the solution for algebraic Riccati equation (22). The Hamiltonian matrix is given as follows [19]:

$$HM = \begin{bmatrix} A(\mathbf{x}) & -B(\mathbf{x})R^{-1}B^T(\mathbf{x}) \\ -Q(\mathbf{x}) & -A^T(\mathbf{x}) \end{bmatrix}. \quad (24)$$

Hamiltonian matrix HM has a size of $2n \times 2n$, where n is the dimension of vector $\mathbf{x}$. The Hamiltonian matrix has symmetric eigenvalues in the complex plane. For these

systems a stabilizing solution exists if and only if *HM* has 2*n* eigenvalues with negative real part. Using corresponding eigenvectors of these eigenvalues (22) can be solved for matrix *P*. Using corresponding *2n* eigenvectors one can construct the following matrix:

$$\begin{bmatrix} \vdots & \vdots & \vdots & \vdots \\ \lambda_1 & \lambda_2 & \cdots & \lambda_n \\ \vdots & \vdots & \vdots & \vdots \end{bmatrix} = \begin{bmatrix} Y \\ X \end{bmatrix}, \tag{25}$$

Then finally, the SDRE solution can be calculated as follows:

$$P = XY^{-1}. \tag{26}$$

Using the calculated matrix, *P* the control (23) can be obtained.

C. Matrices for coupled motion equations

Obtaining the matrices *A* and *B* are of a great importance for SDRE-based approach. As already mentioned there is no unique way to determine them. In this paper, the factorization is performed in a way to achieve the controllability of pair *A* and *B*. The state vector $\mathbf{x}(t)$ has 12 components. The state vector is composed of three vector-part quaternion components (q_1, q_2, q_3), the angular velocity vector $(\omega_x, \omega_y, \omega_z)$, relative translational position and velocity of docking points $(x, y, z, \dot{x}, \dot{y}, \dot{z})$. The control vector $\mathbf{u}(t)$ contains six elements to provide a full feedback control for the coupled motion. The three first elements of vector $\mathbf{u}(t)$ are reaction wheels control vector $\dot{\mathbf{h}}_{WC}$ and thrusters force vector $\mathbf{F}$.

The state matrix *A* is chosen in the following form:

$$A = \begin{bmatrix} \begin{bmatrix} sk(M^T\boldsymbol{\omega}^D)_{3\times3} & q_4 M^T_{3\times3} \\ 0_{3\times3} & Ro \end{bmatrix} & 0_{6\times6} \\ 0_{6\times6} & \begin{bmatrix} I_{3\times3} & 0_{3\times3} \\ 0_{3\times3} & CLW \end{bmatrix} \end{bmatrix}. \tag{27}$$

Here

$$\begin{aligned} \mathrm{Ro} = &-sk(MI_C^{-1}M^T\boldsymbol{\omega}^D)I_C M^T + \\ &+ sk(\mathbf{h}_{WC})MI_C^{-1}M^T - sk(MI_C^{-1}M^T\boldsymbol{\omega}_D^D)I_C M^T - \\ &- sk(\boldsymbol{\omega}_D^D) + sk(I_C M^T\boldsymbol{\omega}_D^D)MI_C^{-1}M^T, \end{aligned} \tag{28}$$

$$CLW = \begin{bmatrix} 0_{3\times3} & I_{3\times3} \\ kI_{3\times3} + W & -2sk(\boldsymbol{\omega}_{OT}) \end{bmatrix}, \tag{29}$$

$$W = \begin{bmatrix} 3\omega_{OT}^2 & \dot{\omega}_{OT} & 0 \\ -\dot{\omega}_{OT} & 0 & 0 \\ 0 & 0 & -\omega_{OT}^2 \end{bmatrix},$$

$$\boldsymbol{\omega}_{OT} = \begin{bmatrix} \omega_{OT}, 0, 0 \end{bmatrix}^T,$$

$$k = -\mu / \sqrt{(r_c)^3},$$

$$r_c = (r + x^2) + y^2 + z^2.$$

For a given vector, the skew-symmetric matrix is defined as follows:

$$sk(\mathbf{M}) = \begin{bmatrix} 0 & -M_3 & M_2 \\ M_3 & 0 & -M_1 \\ -M_2 & M_1 & 0 \end{bmatrix}$$

The control matrix *B* is in the following form:

$$B = \begin{bmatrix} 0_{3\times3} & 0_{3\times3} \\ -DI_C^{-1} & 0_{3\times3} \\ 0_{3\times3} & 0_{3\times3} \\ 0_{3\times3} & Eye_{3\times3}/m \end{bmatrix}, \tag{30}$$

Where $Eye_{3\times3}$ is identity matrix of order 3. Thus, with defined dynamic and control matrices *A* and *B* the SDRE control algorithm can be applied for the rendezvous problem.

IV. Numerical Investigation

In this section the proposed control algorithm performance is studied using numerical simulations. Two different debris shapes are considered the dynamically spherical body and cylinder-like body. In the second case, the matching of the two docking points is more affected by the attitude free motion of the target. It is assumed that the spacecraft is initially close to the debris position The debris orbital parameters and spacecraft initial conditions are presented in TABLE I. The mass of satellite is 50 kg. For the first case, it is assumed the target is spherical object and the moment of inertia of the chaser and the target are $I_C = 2I_T = 2.2\,Eye_{3\times3}\ \mathrm{kg\cdot m^2}$.

TABLE I. SIMULATIONS PARAMETERS

Simulations Parameters			
Orbital elements of the target		***Initial condition***	
Attitude, km	750	$\mathbf{q}_0$	$[0,0,0,1]^T$
Eccentricity	0.03	$\boldsymbol{\omega}(t_0)$, deg/s	$[10,-10,20]^T$
Inclination, deg	70	$\rho_0 = r_0 = [x_0, y_0, z_0]^T$	$[50,27,100]^T$
Right ascension, deg	50	$\dot{\rho}_0 = \dot{r}_0$, m/s	$[0,-2,0]^T$
Argument of perigee, deg	80	Chaser docking point ρ_{i1}, m	$[1,1,0]^T$
		Target docking point ρ_{jo}, m	$[1,0,1]^T$

To implement the SDRE-based control algorithm the following steps are necessary to be accomplished. First is to produce a proper SDC factorization of dynamical system and control that is done in the Section III. Secondly, the State Dependent Riccati Equation must be solved to obtain the positive definite matrix P at each control step. And finally resulted feedback control law is to applied in the closed loop system.

The spacecraft approaches to the debris from a close distance. The reaction wheels installed on the spacecraft are used to compensate disturbance torque caused by the

misalignment of thrusters 2 mm from the center of mass and to perform the attitude tracking maneuver. The debris constant angular velocity is assumed to be known. The spacecraft is controlled to accomplished rendezvous maneuver and attitude tracking simultaneously.

Consider for an example the simulation of the controlled motion with defined above parameters of the system. Fig. 2 shows the relative translational motion of spacecraft during the motion relative to the debris. The trajectories of the motion using uncoupled and coupled dynamical model are presented. Spacecraft reached to zero in the maneuver time Fig. 3 shows the vector-part quaternion components that tend to a zero, so the attitude maneuver is successfully accomplished. Fig. 4 presents the relative angular velocity, which is also converging to zero. The rotational tracking is performed by torques produced by reaction wheels showed in Fig. 5. As the reaction wheels have to maintain the final relative attitude and velocity they have the unloaded angular momentum after the maneuver. Fig. 6 shows the thrusters force produced to control the translational motion. After reaching the debris and make the relative position and velocity, zero; the two objects will have the same orbit. Fig.7 and Fig. 8 shows relative position and velocity of the docking points of the chaser relative to the debris docking point, which converge to zero smoothly.

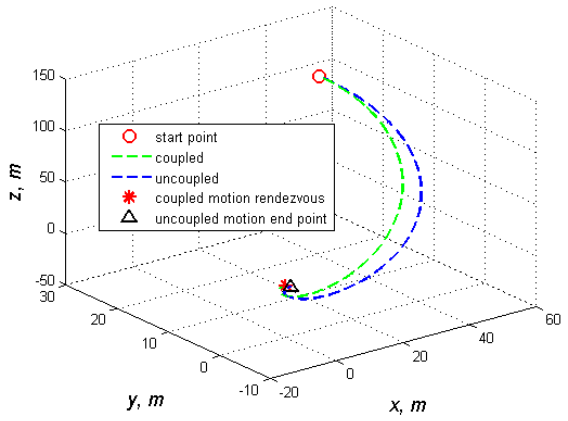

Fig. 2. Translational trajectory of spacecraft relative to the debris

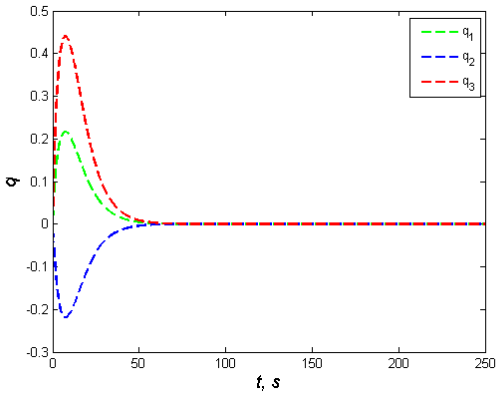

Fig. 3. Vector-part quaternion components

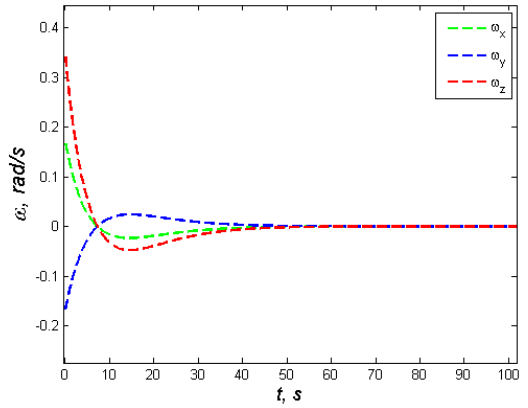

Fig. 4. Relative angular velocity of spacecraft

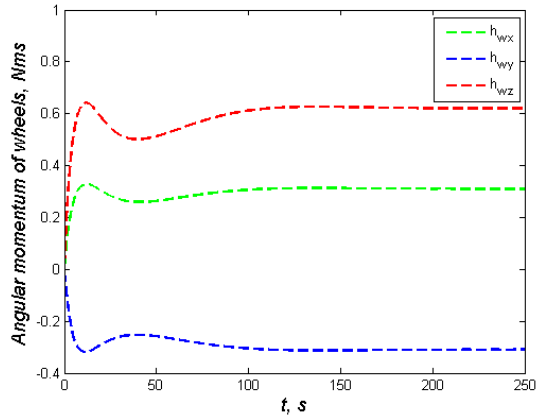

Fig. 5. Angular momentum of reaction wheels

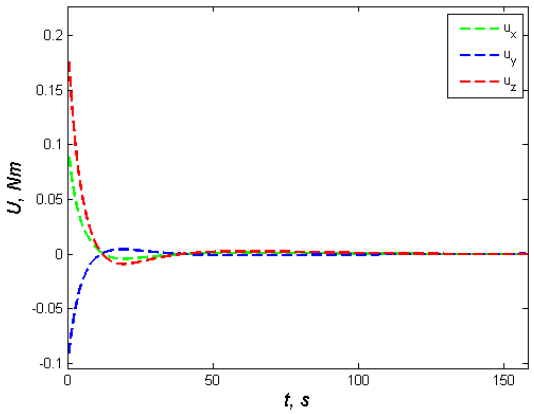

Fig. 6. Thrusters force for translational motion control

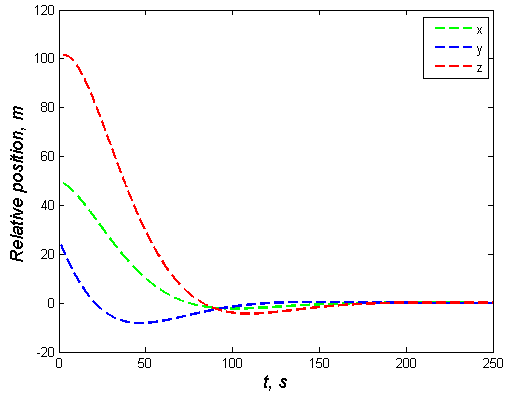

Fig. 7. Position of spacecraft relative to the debris

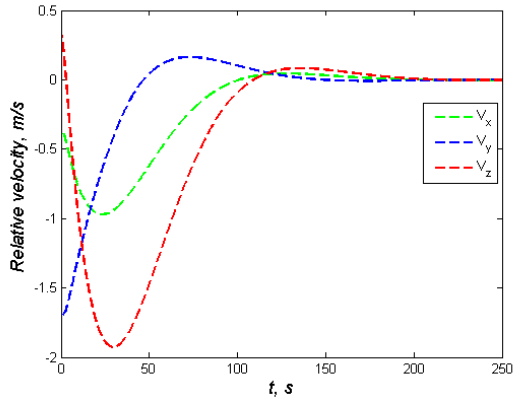

Fig. 8. Relative velocity of spacecraft with respect to the debris

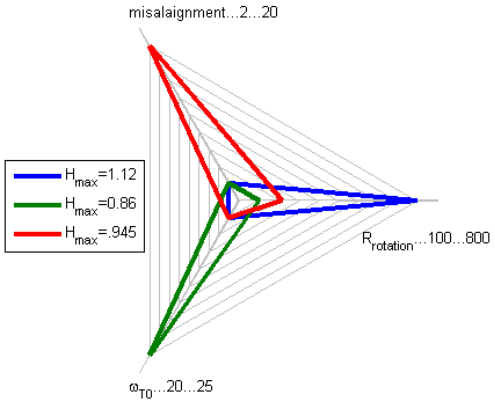

Fig. 9. Schematic dependence of maximum angular momentum of reaction wheels on weighting matrix, debris angular speed, and misalignment of thrusters

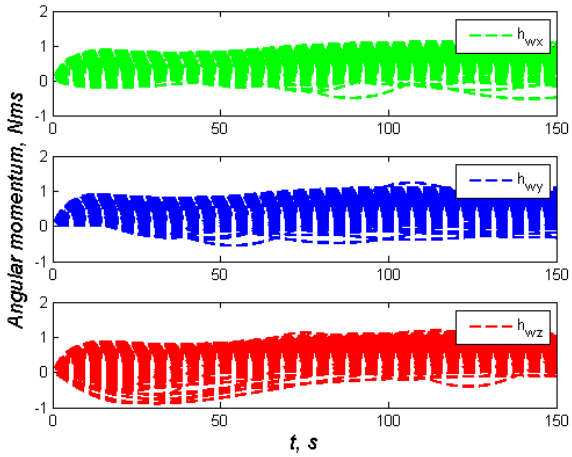

Fig. 10. Angular momentum of reaction wheels for 200 numerical simulations

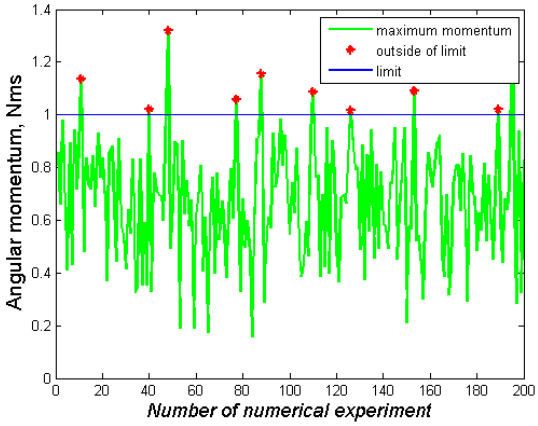

Fig. 11. Maximal angular momentum of reaction wheels for a 200 numerical simulations

Reaction wheels have a maximum possible angular momentum. Consequently, any attempt to produce more than the certain amount will lead to saturation of wheels. Operational area for the reaction wheels for performing the rendezvous should be obtained for the practical considerations. Based on (13) and the control law there are four key parameters which affects performance of reaction wheels during maneuver. It is the initial rotational speed of debris, the weighting matrix of control, the misalignment of thrusters, and finally target moment of inertia that cause the tumbling. Let fix weighting matrix Q as identical matrix, while the weighting matrix R can be algorithm-tuning parameter. The other parameters that affect the angular momentum are defined for the given chaser spacecraft and target object. These parameters is required to be known in advance to predict the feasibility of maneuver. Investigation of the worst possible cases to obtain these parameters constraints for the debris removal mission will help to prevent the situation that reaction wheels are saturated and the capturing will fails.

Let us for the considered system find out the maximum possible values of rotational speed of debris, misalignment of thrusters, and control weighting matrix, at which the reaction wheels will not be saturated after the docking maneuver. Consider first the dynamically spherical target body and set the reaction wheel maximum angular momentum as 1 Nms . Fig. 9 schematically shows areas in which the reaction wheels are still not saturated according to the preliminary numerical study. The acceptable values lie in the following areas $\omega_D^D < 23.9$ deg/s , misalignment ≤ 15mm and $120 \cdot I_{3\times3} \le \tilde{R} \le 200 \cdot I_{3\times3}$, where $\tilde{R}$ is part of the weighting matrix corresponding to reaction wheels control. To obtain these areas a set of random points was chosen for a numerical simulation.

Fig. 10 shows that the arbitrary chosen points lead to acceptable angular momentum values for a defined maximal angular momentum. Fig. 11 shows the maximal angular momentum for 200 numerical simulations (Monte Carlo method) with points in the acceptable area with fixed $H_{\max} = 1$ Nms. However, it can be seen that at some numerical experiments the maximal angular momentum exceeds this limit due to nonlinearity in the motion equations. Nevertheless, these points are in the neighborhood of the critical border.

A new problem arises when the target object is not spherical. Consider cylindrical objects or rectangular cuboid shaped debris with diagonal moment of inertia matrix with different diagonal values. From (13) it can be seen that the term $[\boldsymbol{\omega}_D^D I_D \boldsymbol{\omega}_D^D]$ is equal to zero for the spherical object. In this part it is assumed that the target has a cylindrical shape. In this case the inertial matrix can be written as follow:

$$\begin{bmatrix} I_x & 0 & 0 \\ 0 & I_y & 0 \\ 0 & 0 & I_z \end{bmatrix} = \begin{bmatrix} ratio*I & 0 & 0 \\ 0 & ratio*I & 0 \\ 0 & 0 & I \end{bmatrix} = \begin{bmatrix} m(3r^2+h^2)/12 & 0 & 0 \\ 0 & m(3r^2+h^2)/12 & 0 \\ 0 & 0 & mr^2/2 \end{bmatrix}. \quad (31)$$

The ratio h/r represents the elongation of the target. The bigger the ratio, the more control value along x and y axis should be applied. In this case assuming $h = r$ then $I_{xx} = I_{yy} = 4I_{zz}$ while the other parameters are fixed and have the same value as in the previous case. Fig. 12 and 13 show the quaternions and angular velocity for considered example. These two figures show that the settling time is increased in comparison to the case of dynamically spherical body. The periodical rotation behavior can be seen in Fig. 14, while in the previous case there is no oscillations in the angular momentum of reaction wheels.

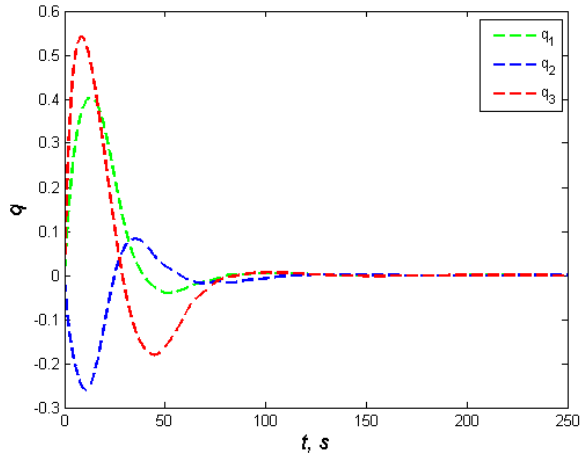

Fig. 12. Vector-part quaternion components

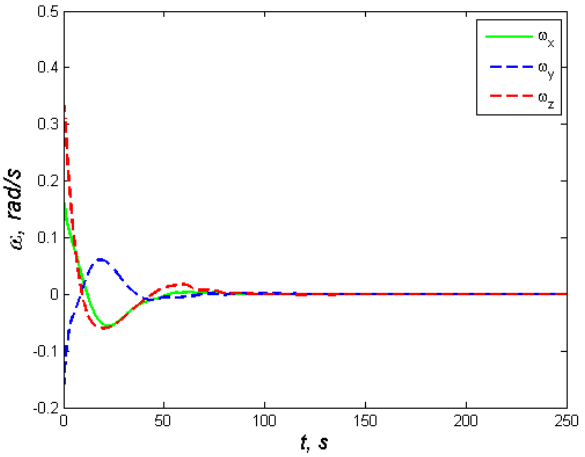

Fig. 13. Relative angular velocity of spacecraft

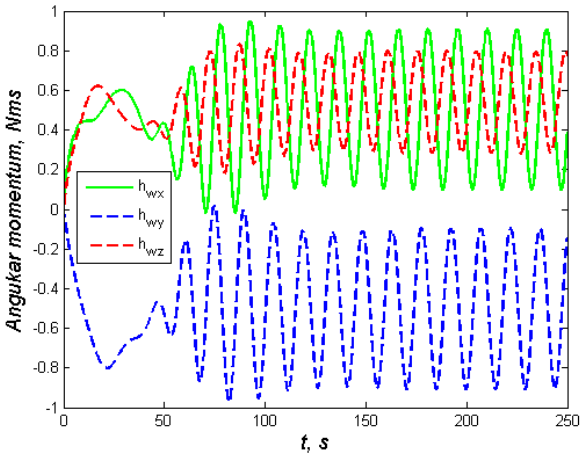

Fig. 14. Angular momentum produced by reaction wheels

It can be obtained that for larger values of h with the chosen reaction wheels the area of the acceptable angular velocity of target reduces. It means that for the similar condition for a spherical body and an axisymmetric body, more angular momentum is needed to be produced by reaction wheels. To obtain this idea. In this work ratio in (31) is assumed to be randomly in the domain ($0.5I_{zz} \le I_{xx} = I_{yy} \le 3I_{zz}$), which represent a cylindrical object. Fig. 15 shows how the new added condition increase the required angular momentum in comparison to Fig. 10. Fig. 16 shows the increased number of critical situation when the maximum angular momentum is outside the value of predefined limit value 1 Nms.

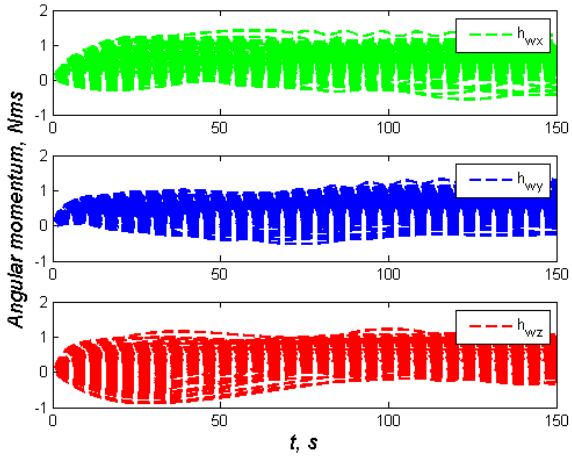

Fig. 15. Angular momentum of reaction wheels for 200 numerical simulations with different choices of moment of inertial

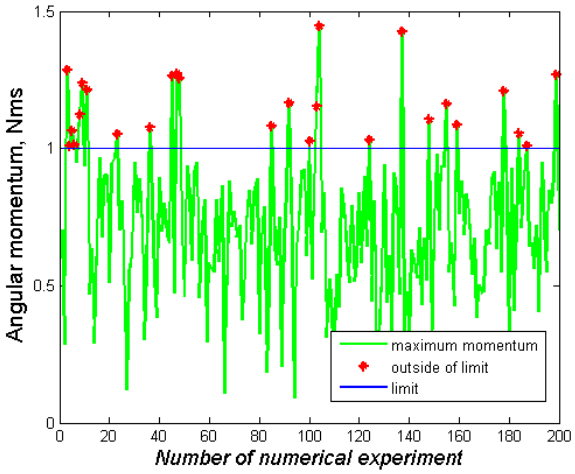

Fig. 16. Angular momentum of reaction wheels for the point in the proposed area

Fig. 17 shows how the increase of ratio affects the required maximum angular momentum. Here the ratio is assumed to be in the interval [0.5; 3] and the other parameter are considered to be in the worst case. One can see that the minimum value of maximum angular momentum is in the case of nearly spherical body when the ration is close to 1. Increasing the elongation of the body (ratio more then 1) or reducing it to a flat body (ratio tends to 0.5) leads to more required reaction wheels angular velocity at the same others simulation parameters.

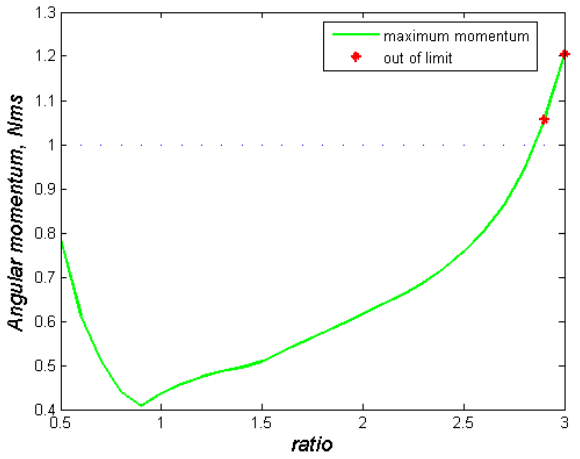

Fig. 17. Effect of moments of inertia ratio on the maximal reaction wheels angular momentum

V. CONCLUSION

In this paper a nonlinear SDRE-based control algorithm for a close range proximity to non-corporative debris is considered. For application of this algorithm aimed to capture the debris at off-center of mass point using a robotic arm the nonlinear coupled relative rotational and translational equation of motion are used. For angular motion control the reaction wheels as the most reliable actuators for attitude control are considered. The dependence of reaction wheels saturation on system and control parameters is obtained. It is shown that the initial angular velocity of target, its inertia tensor are among the critical parameters causing reaction wheels saturation, as well as thruster misalignments and control weighting matrices. The proposed technique allows to determine whether it is possible to track and capture a specific debris with given motion control restrictions of the chaser spacecraft.

ACKNOWLEDGMENT

The work is supported by the Russian Foundation of Basic Research, grant № 18-31-20014.

REFERENCES

[1] M. Shan, J. Guo, and E. Gill, “Review and comparison of active space debris capturing and removal methods,” *Prog. Aerosp. Sci.*, vol. 80, pp. 18–32, Jan. 2016.
[2] C. Bonnal, J.-M. Ruault, and M.-C. Desjean, “Active debris removal: Recent progress and current trends,” *Acta Astronaut.*, vol. 85, pp. 51–60, Apr. 2013.
[3] S.-I. Nishida, S. Kawamoto, Y. Okawa, F. Terui, and S. Kitamura, “Space debris removal system using a small satellite,” *Acta Astronaut.*, vol. 65, no. 1–2, pp. 95–102, Jul. 2009.
[4] V. Aslanov and V. Yudintsev, “Dynamics of large space debris removal using tethered space tug,” *Acta Astronaut.*, vol. 91, pp. 149–156, Oct. 2013.
[5] J. Zhang, K. Yang, and R. Qi, “Dynamics and offset control of tethered space-tug system,” *Acta Astronaut.*, vol. 142, pp. 232–252, Jan. 2018.
[6] B. Wang, Z. Meng, and P. Huang, “Attitude control of towed space debris using only tether,” *Acta Astronaut.*, vol. 138, pp. 152–167, Sep. 2017.
[7] R. Zhong and Z. H. Zhu, “Timescale Separate Optimal Control of Tethered Space-Tug Systems for Space-Debris Removal,” *J. Guid. Control. Dyn.*, vol. 39, no. 11, pp. 2540–2545, Nov. 2016.
[8] S. Estable, J. Telaar, M. Lange, I. Ahrns, M. Theybers, L. Dayers, S. Vanden Bussche, S. Ilsen, R. Lampariello, M. Wygachiewicz, N. Santos, M. Canetri, P. Serra, L. S. Santiago, A. Lukasik, D. Puddephatt, R. Rembala, L. E. Brito, R. Biesbroek, and A. Wolahan, “Definition of an Automated Vehicle with Autonomous Fail-Safe Reaction Behavior to Capture and Deorbit Envisat.,” in *7th European Conference on Space Debris*, 2017.
[9] A. Stolfi, P. Gasbarri, and M. Sabatini, “A parametric analysis of a controlled deployable space manipulator for capturing a non-cooperative flexible satellite,” *Acta Astronaut.*, vol. 148, pp. 317–326, Jul. 2018.
[10] A. Stolfi, P. Gasbarri, and M. Sabatini, “A combined impedance-PD approach for controlling a dual-arm space manipulator in the capture of a non-cooperative target,” *Acta Astronaut.*, vol. 139, pp. 243–253, Oct. 2017.
[11] E. N. Hartley, P. A. Trodden, A. G. Richards, and J. M. Maciejowski, “Model predictive control system design and implementation for spacecraft rendezvous,” *Control Eng. Pract.*, vol. 20, no. 7, pp. 695–713, 2012.
[12] L. S. Breger and J. P. How, “Safe Trajectories for Autonomous Rendezvous of Spacecraft,” *J. Guid. Control. Dyn.*, vol. 31, no. 5, pp. 1478–1489, Sep. 2008.
[13] X. Liu and P. Lu, “Solving Nonconvex Optimal Control Problems by Convex Optimization,” *J. Guid. Control. Dyn.*, vol. 37, no. 3, pp. 750–765, May 2014.
[14] P. Lu and X. Liu, “Autonomous Trajectory Planning for Rendezvous and Proximity Operations by Conic Optimization,” *J. Guid. Control. Dyn.*, vol. 36, no. 2, pp. 375–389, Mar. 2013.
[15] J. Ventura, M. Ciarcià, M. Romano, and U. Walter, “Fast and Near-Optimal Guidance for Docking to Uncontrolled Spacecraft,” *J. Guid. Control. Dyn.*, pp. 1–17, 2016.
[16] M. Sabatini, G. B. Palmerini, and P. Gasbarri, “A testbed for visual based navigation and control during space rendezvous operations,” *Acta Astronaut.*, vol. 117, pp. 184–196, 2015.
[17] D. Ivanov, M. Koptev, M. Ovchinnikov, S. Tkachev, N. Proshunin, and M. Shachkov, “Flexible microsatellite mock-up docking with non-cooperative target on planar air bearing test bed,” *Acta Astronaut.*, Mar. 2018.
[18] T. Çimen, “Survey of State-Dependent Riccati Equation in Nonlinear Optimal Feedback Control Synthesis,” *J. Guid. Control. Dyn.*, vol. 35, no. 4, pp. 1025–1047, Jul. 2012.
[19] M. Navabi and M. R. Akhloumadi, “Nonlinear Optimal Control of Relative Rotational and Translational Motion of Spacecraft Rendezvous,” *J. Aerosp. Eng.*, vol. 30, no. 5, p. 4017038, Sep. 2017.
[20] S. Segal and P. Gurfil, “Effect of Kinematic Rotation-Translation Coupling on Relative Spacecraft Translational Dynamics,” *J. Guid. Control. Dyn.*, vol. 32, no. 3, pp. 1045–1050, May 2009.